Enhancing Thermal Conductivity and Physical Properties of Phenol-Formaldehyde Resin by Adding VGCF during Pyrolysis

Tse-Hao Ko,[1] Hsien-Lin Hu,[1] Wen-Shyong Kuo,[2] Su-How Wang[1]

[1]*Department of Materials Science, Feng Chia University, Taichung, Taiwan*
[2]*Department of Aeronautical Engineering, Feng Chia University, Taichung, Taiwan*

Received 17 May 2005; accepted 3 November 2005
DOI 10.1002/app.23753
Published online in Wiley InterScience (www.interscience.wiley.com).

ABSTRACT: After vapor-grown carbon-fibers (VGCF) were added to resol-type phenolic resin, their influence on microstructure, thermal conductivity, flexural strength, and physical properties of the resin was characterized in this work. Resin with content 0–10 wt % VGCF was heat-treated at 230–2500°C. As a result, it was observed that adding VGCF into resin during pyrolysis not only reduced weight loss but also limited shrinkage of resin. Moreover, adding VGCF to resin promoted the degree of arranging carbon basal planes and chemical densification of the structure of final heat-treated resins. At 2500°C, the graphitized resin with 10 wt % VGCF enhanced flexural strength and thermal conductivity over 300%, while decreasing weight loss around 20% versus graphitized phenol-formaldehyde resin developed from the original resin. © 2006 Wiley Periodicals, Inc. J Appl Polym Sci 102: 1531–1538, 2006

Key words: resins; vapor-grown carbon-fiber; mechanical properties; microstructures; physical properties

INTRODUCTION

In general, a carbon/carbon (C/C) composite material consists of a carbonaceous matrix reinforced by carbon fiber in the form of continuous filament yarn, cloth, chopped fiber, or three-dimensional woven reinforcements. C/C composites are usually formed by pyrolysis of the fiber/precursor composite at temperatures decomposing the matrix precursor. Degradation of polymer precursor is connected with large volumes of gases evolving during pyrolysis; composite counteracts matrix shrinkage and thereby causes cracking of C/C composites.[1] Matrix microstructure affects the overall performance particularly, along with mechanical and heat conduction properties of C/C composites.

Synthetic resins and tar pitch have been used as the matrix precursor for C/C composites. Phenolic resins serve as matrix precursors in C/C composites, since they are relatively easy to use for impregnating fibers, and a large technology base exists from their use in conventional composites processing.[2] Carbon yields from resins that cyclize, condense, and are readily converted to carbon normally range from 50 to 60% by weight. Initial void structure from the matrix significantly influences the mechanical properties of resultant C/C composites.[3–9] Matrix microstructure plays a vital role in deciding overall performance and particularly mechanical properties of C/C composites.[5–12] In view of this, numerous studies have been carried out to control microstructure and degree of graphitization of the matrix to obtain the desired properties.[2,3,13]

Improved mechanical properties of C/C composites were obtained earlier by using phenolic resin graphite powder.[14] Adding (5–10 wt %) small amounts of graphite powder to matrix precursor improved the strength of final composites with non-surface-treated fiber. However, their flexural strength decreased as the amount of graphite powder was added beyond 10 wt %. After 10 wt % graphite powder was added, flexural strength for graphitized composites with non-surface-treated fibers rose from 212 to 293 MPa. Under these conditions, flexural strength for graphitized composites with surface-treated fibers maintained at 587 MPa. C/C composites have also been prepared by addition of 4–20 wt % of inorganic filler ($MoSi_2$).[15] Adding $MoSi_2$ to the composites effectively raised degree of graphitization and bolstered the mechanical properties. Flexural strength for resultant composites with 20 wt % $MoSi_2$ (graphitized at 2300°C) improved from 200 to 360 MPa; we thus expect enhancing microstructure and mechanical properties for a matrix to improve mechanical and physical properties of resultant C/C composites.

Correspondence to: T.-H. Ko (thko@fcu.edu.tw).
Contract grant sponsor: National Science Council; contract grant number: NSC93–2216-E-035–001.

TABLE I
Properties of PYROGRAF III™ Fibers[a]

Property	Value
Fiber diameter	3–20 (μm)
Density	2.1 (g cm^{-3})
Tensile strength	7.0 (GPa)
Tensile modulus	600 (GPa)
Coefficient of thermal expansion	−1.0 (ppm/°C)
Electrical resistivity	55 ($\mu\Omega$ cm)
Thermal conductivity	1950 (W m^{-1} K^{-1})

[a] Source: Applied Science.

Thermal properties of VGCF composites have not been as widely studied. Patton et al.[16] showed thermal conductivity of VGCF composite with acrylonitrile-butadiene-styrene (ABS) and epoxy matrices with an increase in the fiber loading. As VGCF increased from 7.1 to 39.2% by volume, thermal conductivity improved over 260% for VGCF/ABS system and over 250% for VGCF/epoxy system. Gordeyev et al.[17] used polypropylene (PP) filled with VGCF (0–15 vol %), reporting electrical resistance and thermal conductivity with increased fiber loading. Thermal conductivity improved from 0.3 to 1.7 W m^{-1} K^{-1} for 15 vol % VGCF/PP system. The C/C composites with VGCF having both uni- and bi-directional fiber reinforcement, plus different fiber volume fraction ranging from 25 to 56% were prepared by Ting,[18] who found that when composites were heat-treated at 2800°C, fiber loading, composites with varying VGCF loading (25–36 wt %) were prepared to evaluate the ablation, mechanical, and thermal properties of the resultant composites. Thermal conductivity of resultant C/C composites with 36 wt % VGCF added rose from 20 to 502 W m^{-1} K^{-1}. Patton et al.[19] reported changes in physical traits of C/C composites after 0–45 wt % VGCF was added into C/C composites at 1630°C. They also saw thermal conductivity rising from 0.28 to 0.57 W m^{-1} K^{-1} as VGCF amount increased from 0 to 45 wt %. In this study, vapor-grown carbon-fiber (VGCF) as filler was added to the matrix to improve mechanical and thermal qualities of final C/C composites. We also described physical, mechanical, and thermal properties of resin, discussed and related to structure and microstructure of composites after small amount VGCF as filler were mixed into a phenolic resin and then carbonized at temperatures of 600–2500°C.

EXPERIMENT

Resole-type phenol-formaldehyde resin supplied by Chang Chun Petrochemical Industries, Taiwan, was in solution with 60 wt % solid content. Vapor-grown carbon- fiber (VGCF), Pyrograf-III^{TM}, purchased from Applied Science. VGCF properties appear in Table I. A matrix was prepared via adding 5–10% VGCF by weight to resin; 5–10% VGCF by weight was merged with resin, then mixed homogenously by a mixer. Polymer composites were cured at 80°C for several minutes and later hot-pressed at 30 kg cm^{-2} and 120°C for 30 min and 160°C for 10 min. Cured composites were cut to proper size ($80 \times 10 \times 4$ mm^3) and samples pyrolized at a heating rate of 0.5°C/min to 600, 1000, 1800, and 2500°C, respectively. Heat-treated C/Cs were labeled R0, V5, and V10 with 0, 5, and 10 wt % VGCF added, respectively.

A Model 8536 Diano X-ray diffractometer, providing Ni-filtered Cu Kα radiation, measured crystalline-related characteristics of samples. Step-scan method designated d spacing and stacking size (L_c, stacking height of layer planes). Step-interval was set at 0.02 degrees, d spacing and L_c calculated using eqs. (1) (Bragg equation) and (2) (Scherrer equation), respectively:

$$n\lambda = 2d \sin\theta \tag{1}$$

$$L_C(002) \text{ (in nm unit)} = K\lambda/B \cos\theta \tag{2}$$

where $\lambda = 0.1542$ nm; K is apparatus constant (=1.0) and B is half-width of maximal intensity of the peak associated with (002) reflection.

Raman spectrometer was a Renishaw instrument with a Raman imaging microscope system 2000; a 514.5 nm line of an argon ion laser was used as incident radiation. Samples were analyzed with no treatment or preparation, scattered light by the double-grating monochromator, and detected by a cooled photomultiplier tube.

Flexural strength of composites was measured by the three-point bending method prescribed by ASTM D790. According to this standard, the cross head speed is 1 mm min^{-1} during bending procedure and illustration of tree-point bending test is shown in Figure 1. Fractured surfaces of composites were evaluated under a scanning electron microscope (SEM).

Weight loss of composites was determined as follows:

$$W_2(\%) = \frac{W_0 - W_1}{W_0} \times 100\%$$

where W_0 is the original weight, W_1 is the weight after carbonization, and W_2 is the weight loss.

The Archimedes method was used to ascertain density. Open porosity of composites were measured according to ASTM D570; samples were dried in an oven for 1 h at 105–110°C and their weight (W_i) noted. Then samples are placed in a container of distilled water at a temperature of (23 ± 1)°C for 24 h. After immersion for 24 h, these samples were removed from the water one by one, all surface water wiped off with dry cloth,

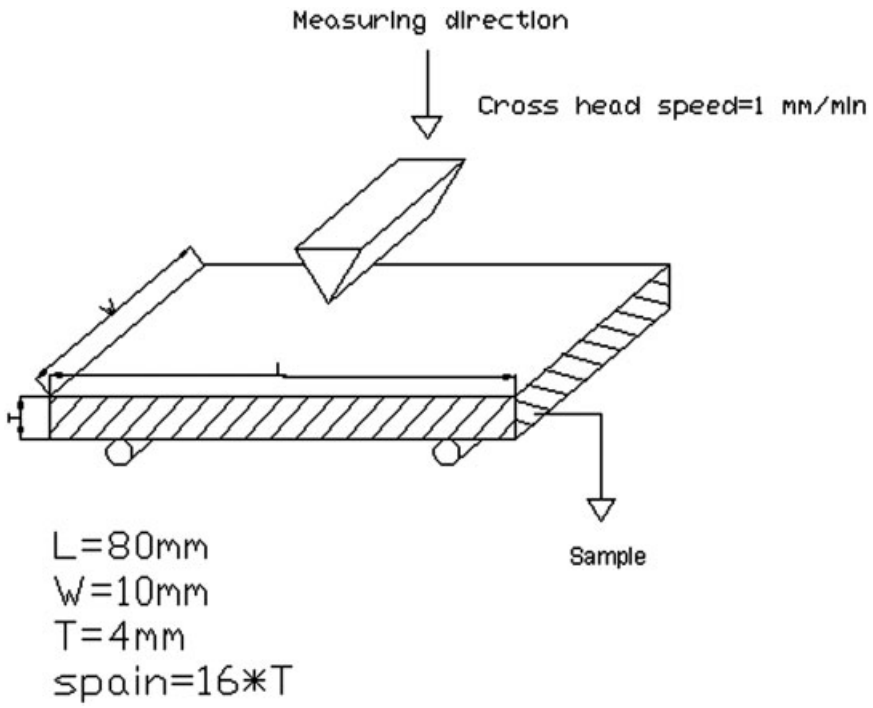

Figure 1 Illustration of the three-point bending test.

and the weight of these samples were recorded again (W_n). Open porosity of composites is determined by:

$$\text{Open porosity (\%)} = \frac{W_i - W_n}{W_i} \times 100\%$$

RESULTS AND DISCUSSION

Weight loss and linear shrinkage

Figure 2 plots variation in weight loss of samples during heat-treatment, calculated from variance in weight of cured and heat-treated samples. During pyrolysis, noncarbon elements in resin were removed as volatile (H_2O, CO, CO_2, H_2, and other gases).[20,21] VGCF was heat-treated above 2500°C before this study, such that VGCF showed no change in weight during pyrolysis. Variance of weight emanates from volatilization of gas from resin: significant below 1000°C, near 100% at 1800°C, in that aromatic ribbon molecules in resin condensed and species of low molecular weight were volatilized. The reactions also shrank resins during pyrolysis (Fig. 2); amount of evolved gas from heat-treatment at 230–600°C was more than 60% of that evolved during pyrolysis. At this stage, condensation and crosslink reactions occurred in resin. Polymeric structure in the original resin was slowly transferred into glassy carbon with suitable mechanical properties. For samples heat-treated at 2500°C, weight loss was 37.3% for Sample R0, 34.1% for V5, and 32.2% for V10.

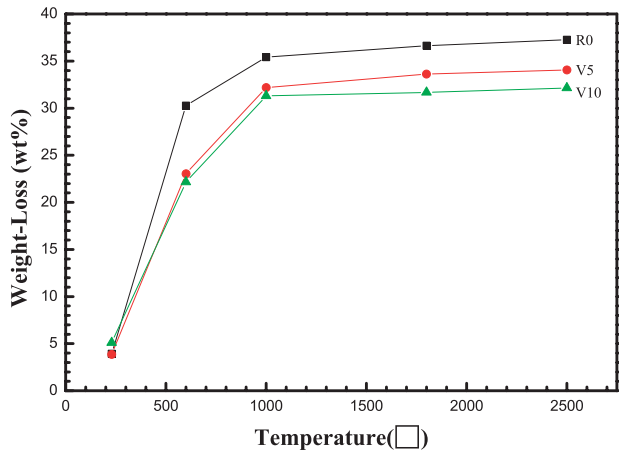

Figure 2 Effect of VGCF addition on weight loss of resins during pyrolysis. [Color figure can be viewed in the online issue, which is available at www.interscience.wiley.com.]

Compared with the behavior of weight loss, linear shrinkage occurred continuously above 1000°C (Fig. 3). Linear shrinkage below 1000°C versus 1000–2500°C happened for different reasons. Below 1000°C, the shrinkage linearly increased with temperature due to condensation and crosslink reactions of polymeric structure to form glassy carbon. Above 1000°C, shrinkage was very slow for all samples. This was attributed to repacking and crosslink of the glassy carbon structure. At 2500°C, linear shrinkage was 17.4% for Sample R0, 15.4% for V5, and 14.5% for V10.

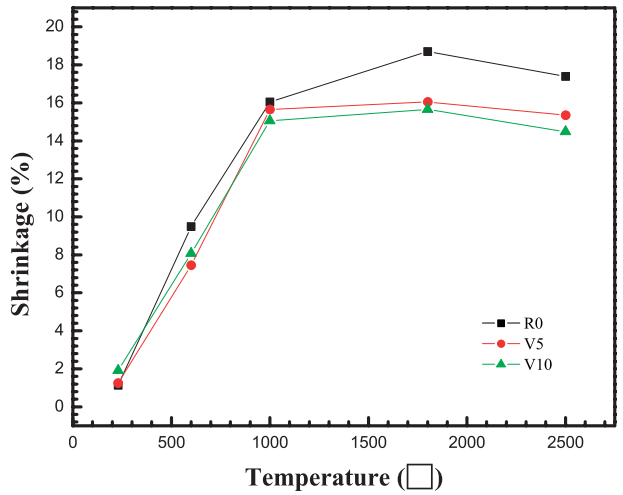

Figure 3 Effect of VGCF addition on linear shrinkage of resins during pyrolysis. [Color figure can be viewed in the online issue, which is available at www.interscience.wiley.com.]

From the studies of weight loss and shrinkage, microstructure of glasslike carbon could be changed by adding VGCF, which was observed to retard polymerization of resin as well as weight loss, and limit linear shrinkage during heat-treatment. The decrease in weight and shrinkage was noticed with great addition of VGCF. Because VGCF was graphitized at 2500°C, it proved to be quite stable during pyrolysis (up to 2500°C), such that the degree of change in weight loss and shrinkage of those samples correlate negatively with the amount of VGCF. At 2500°C, weight loss and shrinkage of Samples V5 and V10 improved by about 14 and 17% over that of R0.

Density and open porosity

Figure 3 shows variation in density of resin during pyrolysis. Two factors affected density of resins during heat-treatment: (1) closed pore formation and (2) chemical densification wrought by chemical structure changes in resin during pyrolysis. This formation of closed pores lowered density of heat-treated resins. At the early stage of pyrolysis of resins, because of condensation of polymeric structure, evolved gases created numerous pores in heat-treated resins. Below 600°C, density of Sample R0 rose to 1.260 g cm^{-3} from 1.243 g cm^{-3}, owing to the effects of chemical densification higher than formation of closed pores. But for Samples V5 and V10, because VGCF is stable at this heat-treatment stage, resin shrank away from the surface of VGCF and formed closed pores, lessening the density and open pores (Fig. 4). Above 600°C, polymeric structure of the resin gradually transformed into the glassy carbon structure; evolved gases could pass easily through pre-existing pores without further volume expansion. At this stage, effect of chemical densification was higher than formation of new pores during pyrolysis. These reactions raised the density of all samples; at 1000°C, maximal value was reached.

Heat-treating temperature affected the density of samples; at 1000–1800°C, density fell with rising temperature because of microstructure rearrangement and formation of closed pores from open pores. At this stage, effect closed pore formation exceeded chemical densification, lessening real density of all samples. Above 1800°C, density increased again due to chemical structure change, condensation, and crosslinkage of the carbon basal phase in resin. With treatment temperature of 2500°C, real density of Samples R0, V5, and V10 was 1.48, 1.54, and 1.52 g cm^{-3}, respectively.

Figure 5 shows variation in open porosity during pyrolysis of different resins. After the curing process, open porosity was 0.99, 0.58, and 0.62% for Samples R0, V5, and V10, respectively. Open porosity of the composite increased rapidly below 1000°C. At 1000°C, open porosity for R0, V5, and V10 was 16.1, 15.7, and 15.1%, respectively. Weak bonding between VGCF and resin meant formation of open pores was enhanced and shrinkage of resin unlimited during pyrolysis. Open pores of resins with VGCF were thus fewer than those of the original resin above 1000°C. At 1000–1800°C, heat increased the microcracks and promoted formation of closed pores,[13,20–22] hence decreasing the open pores. Such aromatization, crosslinking of heterocyclic rings, plus lengthening and broadening of carbon basal planes resulted in repacking of resin structure. These reactions led to conversion of open to closed pores and lower density. At 2500°C, open porosity of Samples R0, V5, and V10 was 0.24, 0.37, and 0.51%, respectively. Weak bonding between VGCF and resin promoted formation of

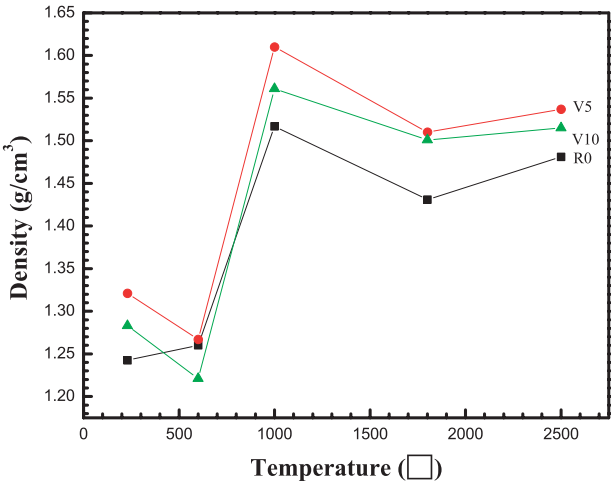

Figure 4 Effect of VGCF addition on density of resins during pyrolysis. [Color figure can be viewed in the online issue, which is available at www.interscience.wiley.com.]

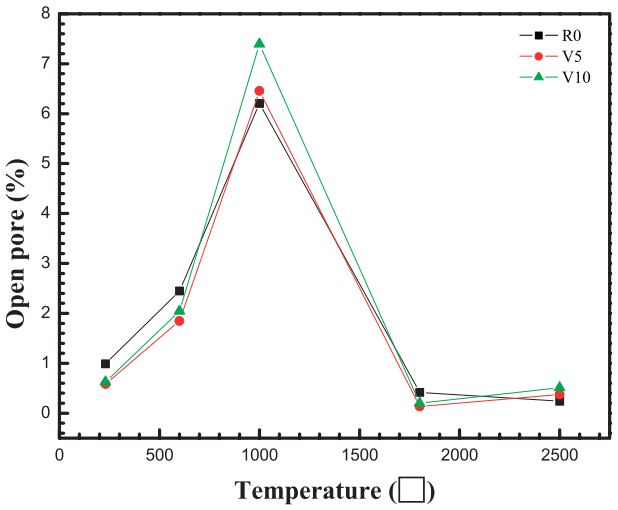

Figure 5 Effect of VGCF addition on open porosity of resins during pyrolysis. [Color figure can be viewed in the online issue, which is available at www.interscience.wiley.com.]

cracks and voids. The original resin thus had fewer open pores than resins with VGCF.

Stacking size, L_c

Figure 6 illustrates variation in stacking size (L_c) of resins during pyrolysis. The L_c of resin climbed very slowly during pyrolysis, indicating that the structure in heat-treated resin as random and disordered. The L_c of resin with VGCF increased very fast due to formation of the ordered structure. Resins with VGCF have greater L_c than original resin during pyrolysis. At 2500°C, the L_c of Samples R0, V5, and V10 was 3.10, 4.41, and 4.96 nm, respectively, indicating that the resin added to VGCF promotes formation of carbon basal planes during pyrolysis.

Raman spectra analysis

Microstructural change of phenolic resin during pyrolysis was characterized by Raman spectroscopy.[23] Above 600°C, Raman spectra showed two strong wide bands near 1580 and 1360 cm^{-1}, as in Figure 7. The peak located near 1580 $cm^{-1}$was due to graphitic structure (D band), and that near 1360 cm^{-1} was due to a disordered structure (G band) in the carbon. It is known that increase of order in carbonaceous materials is reflected by rise in frequency of the G mode as well as drop in frequency of the D mode. It is generally accepted that dependence between the integrated intensity ratio I (D)/I (G) can be deduced by microcrystalline planar size, L_a:

$$L_a = 44[I(D)/I(G)]^{-1}$$

Where I (D) and I (G) are integrated intensities of D and G bands, respectively.

Variation of the L_a of resin increased slightly with temperature up to 1000°C, then more rapidly (Fig. 8). At 1000–2500°C, L_a values rose from 1.20, 2.13, and 2.54 nm to 5.16, 6.15, and 6.99 nm for Samples R0, V5, and V10, respectively.

Compared with L_a, the L_c also grew slowly below 1000°C (Fig. 6), indicating graphite layer planes grew along the *c*-axis to form a crystal below 1000°C. These isotropic structures were small and random. Above 1000°C, the crystal grew not only along the *c*-axis but also along in-plane directions while the characteristic random configuration was maintained.

The microstructure of glass-like carbon could be changed by addition of the VGCF. This study observed that addition of VGCF promoted formation of glass-like carbon. Increase in L_c and L_a of resins with VGCF addition was noted with small addition of VGCF, yet even heat-treated at 2500°C, all samples were still disordered materials.

Mechanical properties

Figure 9 highlights the effects of VGCF addition on flexural strength of resins during pyrolysis. It was found that adding VGCF bolstered flexural strength of resins during heat treatment. The fracture pattern of heat-treated resins showed catastrophic fracture with smooth fracture surface as in Figure 10(a). Flexural strength of heat-treated resin rose by 10% by weight addition of VGCF (Sample V10); failure was catastrophic type with smooth fracture surface, as in Figure 10(b).

During pyrolysis, noncarbon elements in resin were removed as volatiles.[20,21] These reactions led to the

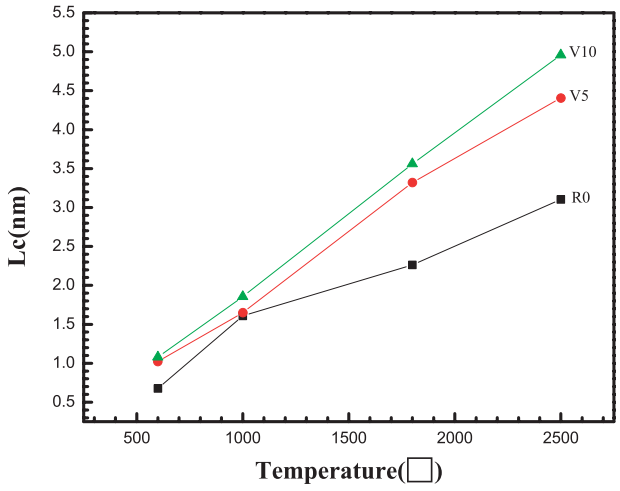

Figure 6 Effect of VGCF addition on stacking size of resins during pyrolysis. [Color figure can be viewed in the online issue, which is available at www.interscience.wiley.com.]

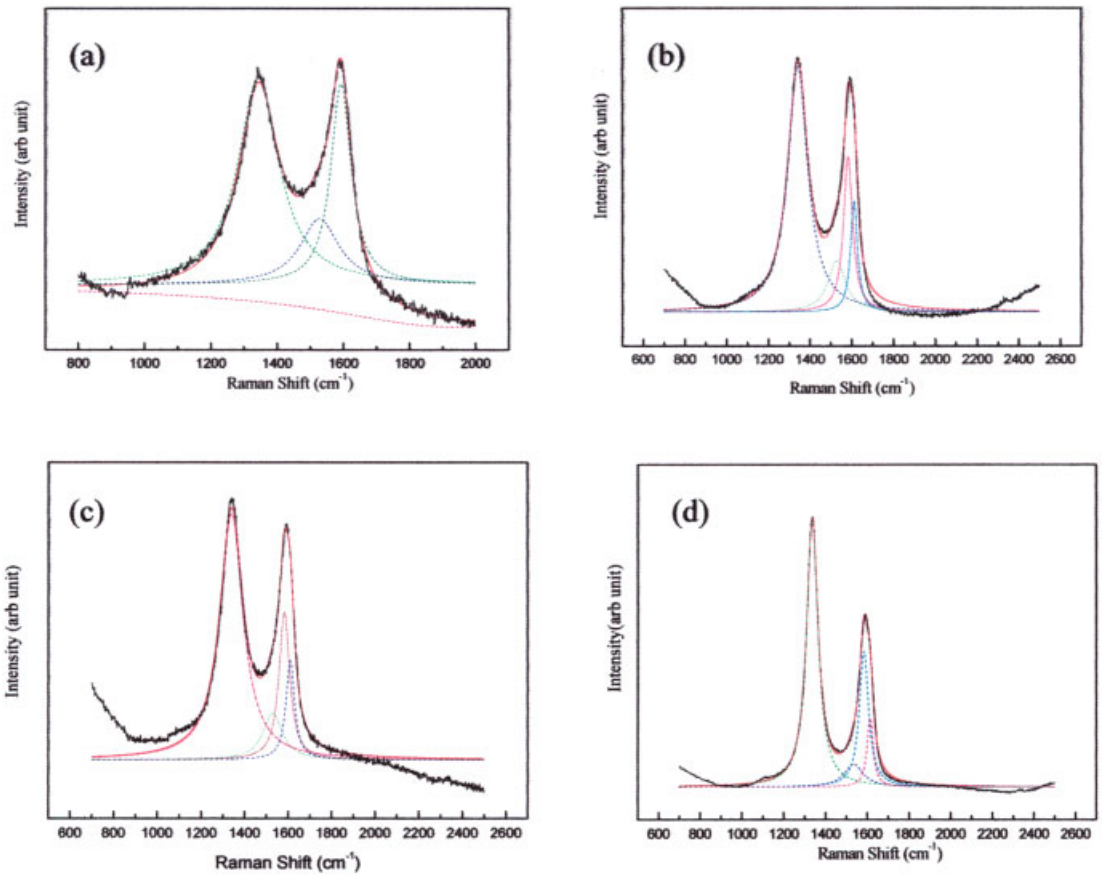

Figure 7 Raman spectra of (a) resin; and (b) resin added 10 wt % VGCF during pyrolysis. [Color figure can be viewed in the online issue, which is available at www.interscience.wiley.com.]

formation of large-size voids as shown in Figure 10(a), plus low flexural strength of heat-treated resins. Formation of carbon layer planes in resin added to VGCF limited shrinkage and formation of open pores, while increasing the density and carbon yield. The large size of voids may lessen flexural strength, but the resins with VGCF had no large voids and hence showed

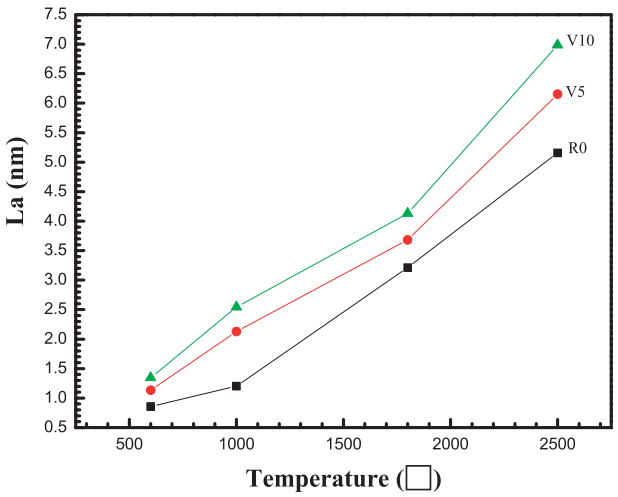

Figure 8 Effect of VGCF addition on L_a of resins during pyrolysis. [Color figure can be viewed in the online issue, which is available at www.interscience.wiley.com.]

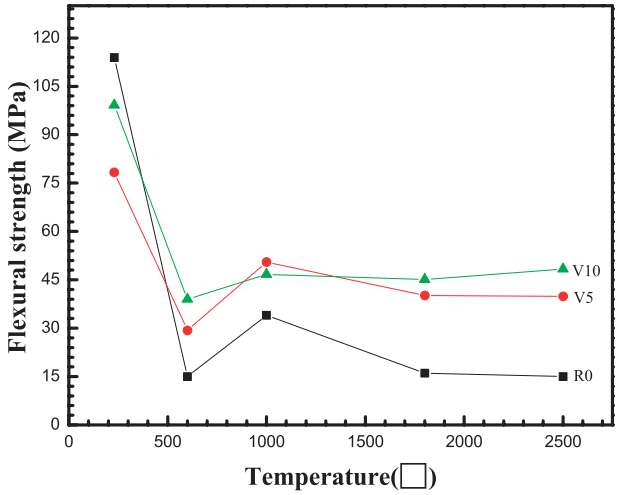

Figure 9 Effect of VGCF addition on flexural strength of resins during pyrolysis. [Color figure can be viewed in the online issue, which is available at www.interscience.wiley.com.]

higher flexural strength than those without it during pyrolysis. At 2500°C, flexural strength of Samples R0, V5, and V10 was 15.0, 40.0, and 48.3 MPa, respectively. Adding VGCF effectively promoted flexural strength of resin during heat-treatment, over 300% with only 10 wt % addition.

Thermal properties

Figure 11 shows that the thermal conductivities of all samples rise with temperature during pyrolysis; effect of VGCF addition on thermal conductivity of resins during pyrolysis is found in Figure 11. After the curing process, thermal conductivity was 0, 0.7, and 1.1 W m^{-1} K^{-1} for Samples R0, V5, and V10, respectively. Two mechanisms exist for thermal conduction in a solid: electrical conductivity and lattice vibration, known as phonons. It was well known how electrical conductivity of resin climbed with temperature during pyrolysis. VGCF fiber thermal conductivity is assumed to be 1950 W m^{-1} K^{-1}, based on known value for Pyrograf III™; that of VGCF/resin composites is assumed to follow the rule of mixture equation, expected value would have been more than 195 W m^{-1} K^{-1} for sample V10 at 2500°C. Experimental data for Samples V5 and V10 is much less than expected, formation of pores in resin is one of reasons for decrease in thermal conductivity. The other reason is that the dispersion of VGCF fiber is not uniform as in Figure 10(b). These reasons yielded lower data than expected. However, at 2500°C, thermal conductivity was 5.0, 13.5, and 15.2 W m^{-1} K^{-1} for Samples R0, V5, and V10, respectively, a rise of over 300% with only 10 wt % VGCF addition.

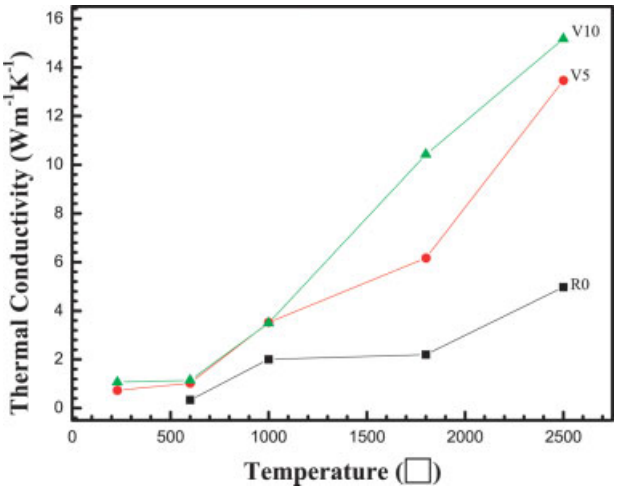

Figure 11 Effect of VGCF addition on thermal conductivity of resins during pyrolysis. [Color figure can be viewed in the online issue, which is available at www.interscience.wiley.com.]

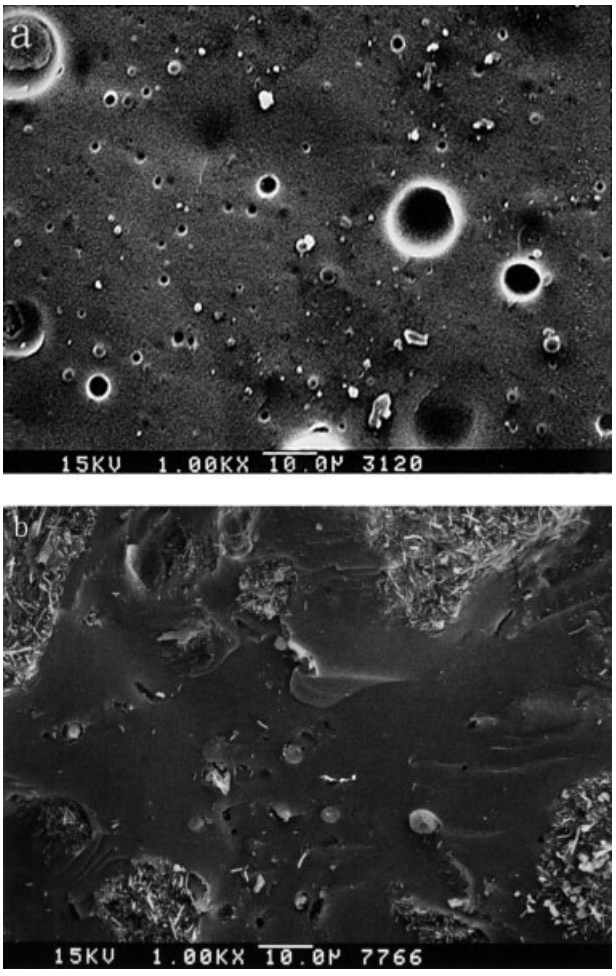

Figure 10 SEM of fracture surface of (a) sample R0; and (b) sample V10, which were heat-treated at 2500°C.

CONCLUSIONS

The above demonstrates how resin additive with VGCF promoted condensation and gas evolution in pyrolysis. This process not only decreased weight loss but also limited shrinkage of the resins with VGCF. At 2500°C, weight loss can be improved by 7–13%. The linear shrinkage of graphitized resin with VGCF exhibited a marked tendency to increase by about 7–17%. Resin additive with VGCF also boosted formation of carbon layers and improved density of final resins. At 2500°C, density of original resin was 1.48 g cm^{-3}; that of resins with VGCF was 1.54 and 1.52 g cm^{-3} for Samples V5 and V10, respectively. The process also reduced open pore formation, L_c of the original resin was 3.10 nm, that of resin with VGCF it was 4.41 and 4.96 nm for Samples V5 and V10, respectively. Heat-treated resins with VGCF showed 300%-plus greater flexural strength and thermal conductivity, developing from the original resin. At 2500°C, flexural strength of original resin was 15.0 MPa, that of resins with VGCF it was 40.0 and 48.3 MPa for Sam-

ples V5 and V10, respectively. Thermal conductivity was 5.0, 13.5, and 15.2 W m^{-1} K^{-1} for Samples R0, V5, and V10, respectively.

References

1. Fitzer, E.; Terwiesch, B. Carbon 1972, 10, 383.
2. Fitzer, E. Carbon 1987, 25, 163.
3. Buckley, J. D. Ceram Bull 1988, 67, 364.
4. Weisshaus, H.; Kening, S.; Siegmann, A. Carbon 1991, 29, 1203.
5. Jain, P. K.; Bahl, O. P.; Manocha, L. M. SAMPE Q 1992, 43, 4347.
6. Manocha, L. M.; Yasuda, E.; Tanabe, Y.; Kimura, S. Carbon 1988, 26, 333.
7. Manocha, L. M.; Bahl, O. P. Carbon 1988, 26, 13.
8. Ko, T. H. Polym Compos 1993, 14, 247.
9. Fitzer, E.; Geigl, K. H.; Huttner, W. Carbon 1980, 18, 265.
10. Kowbel, W.; Shan, C. H. Carbon 1990, 28, 287.
11. Manocha, L. M. Composites 1988, 19, 311.
12. Kowbel, W.; Sham, C. H. Composites 1995, 26, 791.
13. Ko, T. H.; Jaw, J. J.; Chen, Y. C. Polym Compos 1995, 16, 522.
14. Yasuda, E.; Tanabe, Y.; Manacha, L. Carbon 1988, 26, 255.
15. Park, S. J.; Cho, M. S.; Lee, J. R.; Pak, P. K. Carbon 1999, 37, 1685.
16. Patton, R. D.; Piffman, C. U., Jr.; Wang, L.; Hill, J. R. Compos A 1999, 30, 1081.
17. Gordeyev, S. A.; Maodo, F. J.; Ferreire, J. A.; van Haffum, F. W. J.; Bernardo, C. A. Physica B 2000, 279, 33.
18. Ting, J. M. Carbon 1995, 33, 663.
19. Patton, R. D.; Piffman, C. U., Jr.; Wang, L.; Hill, J. R.; Day, A. Compos A 2002, 33, 243.
20. Lum, R.; Wilkins, W.; Robbins, U.; Lyons, A. M.; Jones, R. P. Carbon 1983, 21, 111.
21. Lausevic, Z.; Marinkovic, S. Carbon 1986, 24, 575.
22. Ko, T. H.; Kuo, W. S.; Chang, Y. H. Compos A 2003, 34, 393.
23. Ko, T. H.; Kuo, W. S.; Chang, Y. H. Polym Compos 2000, 21, 745.
24. Shui, X.; Chung, D. D. L. In Proceedings of the 38th International SAMPE Symposium, Anaheim, CA, May 10–13, 1993; pp 1689–1775.